



“Cryogenic Insulation Heat Transfer Model”

A thesis report submitted in partial fulfillment of the requirements for Master of Technology (Gas Engineering).

By,

**M.SreeramaChandra
(R 03020300024)**

Under the supervision of

Dr.B.P.Pandey

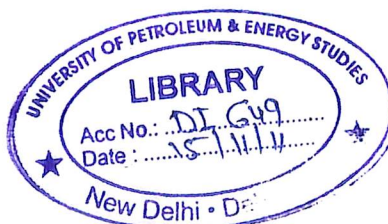
**College of Engineering,
University of Petroleum and Energy studies,
Dehradun-248 007.
May-2005**

UPES - Library



D1649

CHA-2005MT





CERTIFICATE

This is to certify that the Project Report on "*Cryogenic Insulation Heat Transfer Model*" submitted to University of Petroleum & Energy Studies, Dehradun, by **Mr. M. SreeramaChandra** in partial fulfillment of the requirement for the award of Degree of Master of Technology in Gas Engineering (Academic Session 2003-05) is a bonafide work carried out by him under my supervision and guidance. This work has not been submitted anywhere else for any other degree or diploma.

Date: May 30, 05


Dr. B.P. Pandey.

Acknowledgement

Many people have participated directly or indirectly in the preparation of this report, but I would like to express my gratitude's to a few for their valuable contribution.

I owe special debt to **Dr. B.P.Pandey** (Dean), who has been the constant inspiration.

I am equally grateful to **Dr.Himmat Singh** and **Dr.Saraf** for their Cooperation and advice.

I also thank several others who contributed in their own way to make this report Possible.

M. SreeramaChandra.
UPES
Bidholi Village,
Dehradun-248 007, UA, India
Date:

Contents

	Page No
List of Figures	
Executive Summary	
1. Introduction	
1.1 Cryogenic Insulation	1
1.2 General Considerations	3
1.3 Types of Cryogenic Insulations.	4
1.4. Applications of Cryogenic Insulation.	7
2. Fundamental Heat Transfer Process.	14
2.1. Gas Conduction	14
2.2. Solid Conduction	15
2.3. Radiation.	17
3. Evacuated Multi Layer Insulation	18
3.1. Thermo Physical Properties of Reflective Shields and Spacers	18
3.2. Thermal Properties of Reflective shields	18
3.3. Radiation Properties of Reflective Shields	19
3.4. Normal Heat Transfer	20
3.5. Lateral Heat Transfer	21
4. Test Methods	23
4.1. Boil – Off Calorimetry	23
4.2. Electric Input Method	28
4.3. Indirect Methods	28

5. Heat Transfer Model	30
5.1 Introduction	30
5.2 Transmissivity of Thermal Radiation of Thin Aluminum Layer	31
5.3. Multi- Reflection of Radiation between Adjacent Films	32
5.4. Thermal Radiation from Distant films	34
5.5. Radiative Heat transfer at the Boundary	37
5.6. Energy Balance of the Layer	38
5.7. Experimental Results.	39
6. Conclusion	42

References

List of Figures

Figure 1.1 – Types of Cryogenic Insulation

Figure 1.2 – Thermal Diffusivity

Figure 2.1 – Thermal Conductivities of low Temperature Solids.

Figure 4.1 – Boil off Calorimeter

Figure 4.2- Double Guarded Flat Plate Calorimeter

Figure 4.3- Cylindrical Guarded Boil off Calorimeter.

Figure 5.1- Radiative Coefficients of Aluminum Thin Film

Figure 5.2- Radiative Heat Transfer between the Adjacent Layers

Figure 5.3- Radiative Heat Transfer coefficient of Multi Reflection Between Adjacent Layers

Figure 5.4- Radiative Heat Transfer straight Forward from i th Layer to $i + k$ th Layer.

Figure 5.5- Radiative Heat Transfer from i th layer to $i + k$ th layer ($n > 0$)

Figure 5.6- Multi Reflection of Thermal Radiation at the Cold Boundary Wall

Figure 5.7- Thermal Performance q of MLI and Contact Heat Transfer Coefficient h_c between adjacent layers.

Figure 5.8 – Calculated values of net heat flux by increasing n .

EXECUTIVE SUMMARY

The heat transfer analysis of Multi-Layer Insulation (MLI) studied before does not consider that radiant energy is transmitted through the main aluminum coatings of the insulation films. The radiation heat flux is analyzed only between the adjacent films. The thermal radiation coefficient of thin aluminum coatings studied before shows the radiant energy transmitted through the films is not negligible. If the Transmissivity cannot be neglected, the thermal radiation heat transfer between distant films in the MLI must be considered. There are infinite numbers of different heat transfer paths of radiation in MLI. If the path is classified by the number of films through which the radiation is transmitted the equation of energy of each film can be formulated. As the number becomes large, the thermal radiation attenuates more. Then the equation can be solved and gives the heat flux and the temperature of each film in MLI. The heat transfer in MLI is analyzed for different thickness of aluminum coating.

Chapter 1: Introduction.

1. INTRODUCTION

1.1. Cryogenic Insulation

Thermal insulation had long been a subject of great importance to heat transfer engineers and was indeed one of the major concerns in the early development of heat transfer technology. In the last few decades, however, a multitude of new heat transfer research and developments have moved the subject to stagnant obscurity. Thermal insulation had become a classical subject that was considered by many already well developed and concern only to the manufacturing and design engineers. In the meantime, developments in many new emerging technologies have extended considerably the ordinary temperature range of operation, and have presented a great number of formidable engineering problems at the extreme temperature limits. One major problem has been the application sequent. The past few years have registered an intensive surge of renewed interest in thermal insulation, particularly for high-temperature and cryogenic applications.

Despite common basic features of insulation, such as the use of multiple radiation shields, fibrous, materials or powders, high-temperature insulation (say, for the approximate range of 500 to 2500k) differs in many fundamental aspects from cryogenic insulation (say, for temperatures below 100k). The different temperature ranges dictate the use of different insulation materials and methods that in turn result in fundamentally different thermal-property characteristics as well as transport phenomena. For instance, the multisided (or multilayer) insulation concept is employed in both high-temperature and cryogenic insulation, of all, the detailed heat transfer characteristics is quite different. Furthermore, cryogenic insulation is normally operated under the evacuated condition i.e., moderate or high vacuum, while high-temperature insulation often encounters oxidizing or reducing atmospheres. Surface oxidation and material sublimation is indeed a major problem in high-temperature insulation but not is cryogenic insulation.

Cryogenic insulation is unique in many ways, when compared to insulation for application in other temperature ranges. From the practical viewpoint, it has played and is continuing to play a most prominent role in the field of cryogenics. The importance of

Insulation in cryogenic is easily realized by nothing that the heat of vaporization of cryogenic liquids as well as the specific heats of matter at cryogenic temperatures are much smaller than the corresponding ones at room temperature, and it takes little inflow of heat from outside to boil off the cryogenic liquids or to raise the system. Cryogenic insulation has constituted a giant step in the growth of cryogenic science and technology. The study of cryogenic phenomena become possible only after the discovery of Dewar flasks (or simply Dewar) in 1893. The development of low-cost porous (foam, fiber, or powder) insulation for transportation and storage has been primarily responsible for the large scale use to liquefied gases in industry. In the last ten years, the advances in evacuated insulation, especially the evacuated multilayer insulation, have contributed enormously to the rapid development of rocketry and space exploration programs, liquid helium technology, superconducting technology, and many others.

On the fundamental side, cryogenic insulation has presented a score of new and unique heat transfer problems that have consistently puzzled and troubled heat transfer engineers and have provided great challenges to researchers. In addition to the complex internal geometry involved in cryogenic insulation medium, unique material behaviors at cryogenic temperatures originate heat transfer processes and mechanisms that are uncommon to the conventional thinking and analysis of heat transfer phenomena at moderate temperatures. Moreover, the relatively young field of cryogenic provides ample opportunity for further fundamental research in cryogenic insulation heat transfer. Indeed, a sharp contrast exists today between the importance and wide acceptance to newly develop cryogenic insulation and the lack of fundamental understanding in its heat transfer processes.

The purpose of the present study is twofold: first, to provide the fundamental information necessary for the design and evaluation of the thermal performance of cryogenic insulation, and secondly, to review and assess the existing contributions in the literature for future research in this area. The scope of the present study is limited to those aspects that have direct relevance to the understanding of heat transfer processes in cryogenic insulation. Many other important topics that could affect the thermal performance of cryogenic insulation will not be treated here. These include, for instance,

manufacturing of insulation materials, mechanical supports and penetrations evacuation and purging processes, test standards, systems design, etc.

1.2 General Consideration

Thermal insulation refers to either a single homogeneous material or a mixture of material in a composite structure that is designed to reduce heat flow between their boundary surfaces. The choice of thermal insulation material and structure for a particular application depends on the required thermal effectiveness of the insulation as well as many other factors such as economy, weight, volume, convenience, ruggedness, etc. `due to the extreme-temperature condition and the required ultrahigh thermal effectiveness, cryogenic insulation normally exists in a composite form with combination of material of desired thermal mechanical properties. Various types of cryogenic insulation will be instruction after this subsection.

The inhomogeneous composite structure of cryogenic insulation makes the heat transfer analysis a rather complicated problem. Consideration must be given to the complex interactions of various heat transfer mechanisms in an inhomogeneous medium and in some cases, to the highly anisotropy (i.e., dependent of the heat flow direction) behavior. Heat transfer through cryogenic insulation usually consists of the simultaneous action of the following mechanism: solid conduction through the insulation materials and between individual insulation components across areas of contact, gas (or residue gas under vacuum condition) conduction in void space within the composite structure, and radiation these void spaces and through some of the insulation components.

Because of the complex interactions of various mechanisms, it is practically useful and convenient to define an "apparent" (or "effective" or "equivalent") thermal conductivity to characterize the thermal effectiveness of the insulation. Consider, for simplicity, the one-dimensional case involving slab insulation. The following relation defines the apparent thermal conductivity k_a :

$$Q = k_a A(T_1 - T_2)/L$$

Where Q is the total heat flow through insulation, A the heat-flow cross-sectional area, T_1 and t_2 the boundary temperatures, and L the insulation thickness. For an anisotropic insulation, there will be more than one apparent thermal conductivity. In steady-state operation, the apparent thermal conductivity is the important parameter for the evaluation of thermal effectiveness. The product of conductivity time's density becomes of major importance in certain spacecraft applications because of launch and injection weight consideration. For instance, to design for a specific heat flux q (W/m^2) in the insulation weight w (kg/m^2) is determined as follows:

$$w = \rho L = \rho k_a \Delta T / q$$

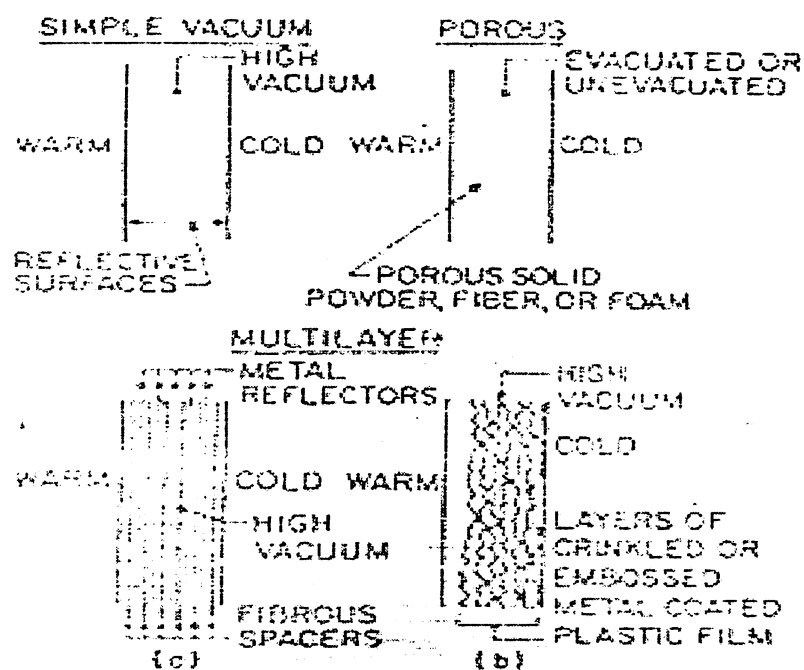
Where ρ is density. To minimize the insulation system weight requires the product ρk_a to be a minimum. Under unsteady conditions such as during cool-downs, warm-ups, and boundary temperature transients, the volumetric heat capacity (i.e., the product of density and specific heat) of the insulation is also an important parameter. The greater the volumetric heat capacity, the longer the temperature response time will be and the larger the heat change that will be required for a change of insulation temperature.

1.3 Types of Cryogenic Insulation

There exist two general classes of cryogenic insulation: the unevaluated and evacuated. The unevaluated insulations are porous materials such as solid foams, powders, and fibers in which the interstitial spaces are filled with gas at atmospheric pressure. The porous structure serves to reduce solid (and in certain instances gaseous) conduction as well as radioactive transfer between boundary surfaces. While the thermal effectiveness of porous insulations is relatively poor as a result of gas conduction, they are widely used in less-demanding cryogenic insulation systems on account of their low installation cost. For systems operating at temperatures below the liquid-oxygen temperature, the insulations normally used are the evacuated ones. The evacuated insulations can be subdivided into three major types: simple high-vacuum insulation, evacuated porous insulation, and

evacuated multilayer insulation. In particular, the last two types constitute the major recent advances in this area and will receive primary attention in the presentation here. Figure below illustrates schematically various types of cryogenic insulation.

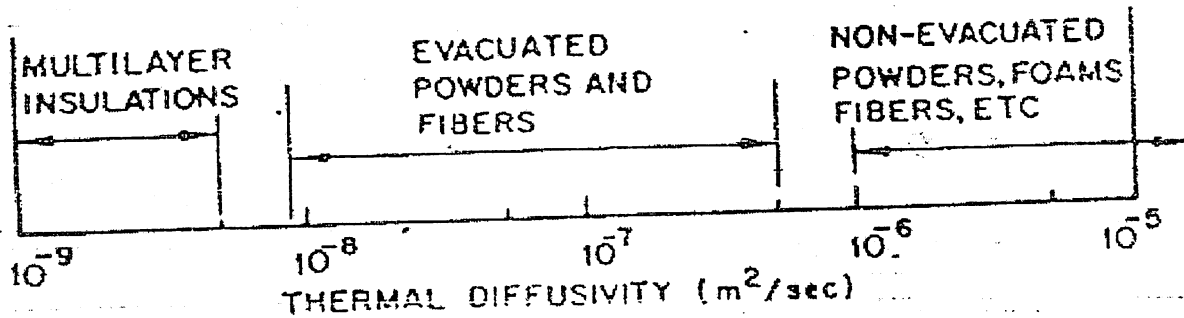
Figure 1.1. Types of Cryogenic Insulation



The simple high-vacuum insulation system is composed of a well-evacuated space bounded by highly reflective walls. The classical Dewar flask and the Thermos bottle both are of this type. It is structurally and conceptually the simplest, has the least weight and least heat capacity, but is not very effective thermally because of the direct radioactive exchange between two bounding surfaces.

Conceptually, the evacuated multilayer insulations are a direct extension of the simple high-vacuum insulation system by merely placing many radiation shields in between two boundaries. They normally consist of a laminated assembly of numerous thin (0.15-3 mils) plastic films coated on one or both sides by a thin vapor-deposited layer (400-Å) of high reflectance metal, usually aluminum or gold. The plastic films are employed instead of solid metal films because of their high mechanical strength, low density, and low thermal conductivity. These radiation shields (10-50 per cm) are separated from each other either by spacers of low thermal conductivity such as low density paper or netting (0.6-6-

mil thick), by crinkling or embossing the shields so that when they are placed against each other they touch only at a few discrete points, or by tufts of short fibers bonded to one surface. As shown in fig.1.2, the evacuated multilayer insulations have the highest thermal effectiveness, and as a result, are often called the "super-insulation." These materials have very low thermal diffusivity (Fig.1.2).



They are, however, the most expensive and difficult to install, and highly anisotropic with the lateral (i.e., parallel to the lamination) apparent thermal conductivity three to six orders of magnitude greater than that normal to lamination. Such a large disparity in directional thermal resistance presents a serious. Thermal design problem for systems where structural members and plumbing lines penetrate the insulation and provide lateral heat at their junctures.

The evacuated porous insulations are essentially the same as the unevaluated insulations except that they are operated under high vacuum conditions. In comparison with the evacuated multilayer insulations, they are isotropic, simpler to install, less expensive, and conductivity is one or two orders of magnitude higher than the normal apparent conductivity of the evacuated multilayer insulations. The unsurpassed thermal effectiveness of the evacuated multilayer insulation, however, may soon be challenged as a result of recent developments in evacuated porous insulations by using packed beds of hollow dielectric spheres coated with highly reflective films.

1.4. Applications of Cryogenic Insulation.

To date, the largest application of cryogenic insulation has been for the storage and transportation of cryogenic fluids on the earth. The liquid cryogens handled in large quantities are liquefied natural gas (LNG), oxygen, nitrogen, and hydrogen, and to a lesser extent helium. Boiling temperatures of these fluids at atmospheric pressure range from 120 to 4.2⁰K. Capacities of storage and transportation vessels are from a few liters to greater than 100 - million-liters, the latter being associated with the LNG industry. Ocean going LNG tankers in the 100-million liter capacity range are in service, and storage tanks at LNG distribution and peak load-shaving plants for utilities are of comparable size. Both stationary and portable vessels in the size range of a few liters to thousands of liters are used for storage of cryogens in laboratories and manufacturing processing facilities such as in the electronics industry. Associated with these installations are insulated plumbing lines which range in size from small diameter transfer lines a meter or two long to large diameter pipe lines whose lengths are measured in kilometers. Insulation used for this broad category include vacuum; both evacuated and nonevacuated foams, fibers, and powders, evacuated spaces containing cooled radiation shields and / or multilayer insulation, and wood or cork board.

Potential applications in the aircraft and aerospace industries have been the impetus for a major portion of the recent advances in insulation technology for cryogenic storage and handling. These have been dictated by stringent requirements for minimum heat transfer and weight with maximum reliability for long unattended periods of use. The largest aerospace vehicle using insulated cryogenic tankage for propulsion is the Saturn vehicle used for the U.S. Manned Space Program. Other applications include oxygen and hydrogen storage for fuel cells and life-support systems (such as the Apollo program), cryogenically cooled scientific space experiments, and cryogenic tankage for future space programs such as the reusable space shuttle orbiter and booster and the Modular Nuclear Vehicle for deep space missions. Typical aircraft applications have been on board oxygen storage for crew systems, and conceptual study programs for development of LO₂/LH₂ and liquid methane fueled hypersonic aircraft.

Finally, a wide variety of insulated devices have been used for developmental studies, such as LN₂ cooled electrical transmission lines and scientific investigations in the laboratory. Examples of these are in the fields of cryogenic properties of materials, superconducting devices, and high-energy physics. Often very sophisticated insulation schemes have been required because of the desirability of attaining extremely low temperatures (below 4 K) and the high cost of a cryogen such as helium or neon. Much use has been made of cooled shields and outer guard vessels containing a less expensive cryogen in conjunction with evacuated insulations.

Many factors enter into the selection of an insulation system for a specific application. For large storage vessels, the cost, maintainability, and reliability are prime considerations. Minimum total cost per unit quantity of stored or transported cryogen may dictate the type of insulation system to be used for a specific vessel. For LNG or liquid nitrogen, satisfactory thermal insulation is typically achieved by using materials such as evacuated powder, granular materials, or unevacuated foams. As an example, a large LNG tanker ship currently in services has a relatively high boil off rate, but this vaporized liquid is used to fuel boilers for propulsion of the ship which is an important factor in the economic choice of the optimum insulation system for this particular application. In most aerospace cases installed cost is not as important a consideration, and minimum heat flux for long-term storage in space or weight including cryogen boil-off, is the prime factor. For launch or booster systems, the storage time requirements are for a few hours, and less efficient insulations may be acceptable. Such is the case of the Saturn vehicle, which used a foamed insulation. In months great care must be taken to assure minimum heat flux into the storage vessel at minimum weight. Multilayer insulations, prime candidates, as the pressure within the multilayer becomes an important consideration and factors such as out gassing from the insulation materials and the venting of these products must be considered. Excessive out gassing with ineffective venting degrades the performance because of the higher interstitial. Also, the out gassing products may deposit on reflective surfaces which will increase the Radiative heat transfer.

Brief descriptions of applications of several types of insulation to ground and space cryogenic systems are discussed in the following paragraph. Major emphasis is placed on

Evacuated foams, powder and fiber and multilayer materials as these are more pertinent in term of heat transfer as discussed in the preceding sections. Multilayer insulations are of particular usage because of their thermal anisotropy and sensitivity to compressive loading, which require the use of special design techniques to achieve optimum performance.

Nonevacuated Insulation

Nonevacuated powder, fiber and foam insulations are used extensively in the construction of large LNG storage tanks. For Polyurethane foam, used for a 110 million liter storage facility reported performance is a boil-off of 0.06% of tank volume per day which corresponds to a heat flux density of approximately 15 W/m².

Expanded Perlite has been used as the insulation in double-walled large LNG storage tanks as well as for smaller Dewar's. A problem encountered when using a loose-fill material such as Perlite of silica is the tendency for the material to settle and compact with the thermal contraction and expansion of the inner tank wall during filling and emptying of the vessel. This results in the formation of voids in the upper regions of the insulation space which increases the heat transfer. One method used to overcome this problem is to place a layer of resilient fiberglass blanket material between the inner wall and the powder or granules fill. The fiber blanket acts as a spring to take up insulation. Perlite also has been used in conjunction with wood and glass fiber mixtures to provide a satisfactory thermal insulation for a large storage tank. In this application Perlite was used for roof and floor insulation with slightly compressed fiberglass blocks in the insulation upon contraction of the inner well.

The S-IVB stage of the Saturn I present an example of the use of a Nonevacuated system for short-term liquid-hydrogen storage. The system selected for this application was low-density reinforced polyurethane foam to the internal wall of the LH₂ propellant tank. A barrier layer was applied to the liquid side of the insulation to retard permeation of hydrogen into the foam. Test data showed that the pressure of hydrogen in the foam increased its effective thermal conductivity by a factor of 2 to 3 over the normal value for this foam. The insulation system was designed to provide effective cryogen storage through

Asent and for 4.5 hr in orbit. Internal foam was selected to prevent air liquefaction during ground hold, provide a higher temperature surface for bonding to the tank wall and minimize tank contraction during filling. The performance of this type of system has been demonstrated by the successful flights of this vehicle in the Apollo program.

Evacuated Powder and Fiber Insulation

Powder insulations such as expanded Perlite, silicon and carbon or charcoal have been used in vacuum jacketed cryogenic liquid storage vessels and transfer lines. Filling the vacuum space with a powder of fiber material reduced the heat transfer over that of a simple vacuum section. A further improvement in thermal performance is realized by opacifying the insulation through the addition of metallic flakes or powders. Also, the use of very small particles reduces the vacuum the mean free path of the gas at higher pressures which reduces gas phase conduction.

Settling can be a problem with evacuated powders, and one method used to overcome this problem is by placing a reservoir at the uppermost point of the tank so that excess material will flow from this volume into any voids resulting from settling. This method has been used on a large transportable 6000-liter LH₂ Dewar having a boil-off rate reported to be about 1.5% of the tank capacity per day. A thickness of 30 cm of Perlite fills the vacuum space of the horizontal, cylindrical tank, and because of the very small pore size and long path length, the evacuations of this powder system to a satisfactory pressure level generally require several days of pumping. Also, the finely divided material has a large surface area, and consequently, moisture desorption can be a problem.

An interesting example of the use of fibrous material is found in which describes a program for the development of permanently evacuated vacuum panel insulation. Several glass fiber paper-type materials were investigated for filling thinner space. The vacuum jacket was flexible so the filler material had to support an atmospheric pressure compressive loading.

Evacuated Multilayer Insulation

Extensive usage has been made of this very low thermal conductivity insulation in the field of cryogenics, particularly for aerospace applications. From a standpoint of heat transfer analysis it presents a complex system by the large degree of thermal anisotropy. A number of analytical and experimental studies have been conducted to determine optimum methods for terminating the multilayer at penetrations or edges exposed to a different thermal environment.

The sensitivity of thermal performance to variations in a compressive load which may be applied to this type of insulation presents another application design problem. Relatively small changes in compressive load, such a 10-100N/m² can increase the heat transfer by a factor of two or more as shown in for three types of multilayer systems. The increase in heat flux is due to the increased solid conduction which may be correlated with pressure as shown by the equations fitting the experimental data. Variations in compressive loading of this order of magnitude can readily result from application of the insulation around a sharp corner small-radius surface. Another design problem area is in the attainment and maintenance of a very low gas pressure with in the insulation.

All of these design problems contribute to a large uncertainty in the thermal performance of a given system when installed on a tank or component, and it is obvious that in order to achieve the highest thermal efficiency of this system with a predictable degree of certainty careful design and fabrication procedures must be followed. Typically, uncertainty factors of two to four are used to predict installed insulation performance based upon calorimeter test data of the multilayer material. However, even with this large uncertainty the performance of multilayer insulated systems is significantly better than that the opacified powders.

Multilayer insulations have been used for very efficient ground storage Dewar's for liquid hydrogen and helium. In this type of application the problem of maintaining an adequate vacuum for very long periods of time is not important as the insulation space may be pumped periodically. In many cases, however, the devices are transportable and the inner tank must be supported in a manner which will not excessively degrade thermal

performance and yet can withstand the loads encountered in highway, rail, or air transportation. An example of the application of multilayer insulation to a moderate sized storage vessel is that of a 3000-liter Dewar for storage of slush hydrogen in a laboratory test facility. The cryogen container of this vessel was a vertical cylinder approximately 1.4-m I.D. by 6.7-m high with hemispherical ends. The inner tank was supported to the bottom of the outer shell through tubular fiberglass struts and a cone attached to the outer shell with a sliding cylindrical supporting surface at the inner tank to accommodate thermal contractions and expansions of the vessel. The fiberglass support struts and cone, and all intervessel plumbing lines were insulated with three overlapping multilayer insulation blankets. Total thickness of the combined multilayer blankets was approximately 2.54cm. The multilayer blankets were prefabricated in oversized gars and polar caps for the inner vessel heads, and in oversized rectangular sections for the cylindrical shell. These blanket sections were then trimmed to fit at close tolerance butt joints during installation. Each multilayer blanket section consists of seventeen 0.15-mil double-aluminized crinkled Mylar radiation shields separated by sixteen Tissuglas spacers. During fabrication, all blanket sections were covered on both faces with Dacron mesh to improve handling characteristics. The cylinder blanked sections were further reinforced in the vertical direction with Dacron Rid don, 1.27-cm wide, spaced on approximately 20.3-cm centers and sewn to the mesh net. The composite sections were then fastened together with molded nylon button retainer's spaces approximately 15.2cm on centre. During installation, the cylinder blankets were suspended from the support cone at the top of the Dewar using the Dacron ribbons, the lower gore and polar cap blankets were subsequently attached to the cylinder blankets with aluminized Mylar tape and Dacron thread. Adjacent cylinder and gar sections were attached at the butt joints using Teflon tabs and aluminized Mylar tape.

Measured equilibrium heat transfer to the cryogen Dewar was 17.5 W. approximately 35% was attributed to supports, 15% to plumbing and the remainder to the insulation. Laboratory data on insulation heat transfer were used and degraded by a factor of 2 to account for joints between blankets and buttons supporting the layer in each blanket. The heat flux density for this insulation system was computed to be 0.51 W/m² which for the test temperature conditions corresponded to an insulation effective thermal conductivity

of $5.0 \times 10^{-6} \text{ W/m}^2$. This is compared to the laboratory test value of for the same boundary temperature conditions.

A further improvement on the evacuated, multilayer insulation storage vessel concept has been achieved by incorporation into the insulation space a shield cooled by gas vaporized from the cryogen. Dewar of this type for liquid helium storage has shown significant reductions in storage losses for both liquid helium and nitrogen. Test data shown a factor of 16 reductions in cryogen loss for LHe and a factor of 3 for LH₂. A cooled shield in conjunction with evacuated multilayer insulation has also been incorporated into a solid cryogen refrigerator used to provide one year of cooling for an experiment on a spacecraft. This unit uses two solid cryogen, and the shield is thermally attached to the tank containing the cryogen of higher sublimation temperature in this case carbon dioxide. Argon was used to provide cooling for an infrared sensor and the carbon dioxide container intercepted the thermal energy from the structural members supporting the tank assemblies. The copper shroud is attached to upper tank and enclosed the argon tank at the interior surface of the insulation. A gold-plated, floating radiation shield was suspended between the shroud and argon tank.

A major problem in the application of multilayer insulation to small storage vessels is the contouring to insulate effectively the ends of the container. In some cases this is done by cutting gores for each layer and then overlaying and closing each gore with aluminized Mylar tape. This is a very time-consuming procedure, and if not done with care the insulation performance can be severely degraded by openings at joints or local compression due to excessive overlaps. One method that has been used to simplify insulation of curved surface to apply "shingle" type of multilayer in modules. A partial insulation 1.5-m diameter tank for illustration for this concept. Layers of a crinkled 3-mil single aluminized Mylar was bonded to a Dacron fabric sub layer and a Dacron net outer layer. The Mylar materials is cut in shingle patterns and bonded at each edge to the Dacron fabric and net. The completed module is then attached to the tank with adhesive or nylon fasteners. The effective thermal conductivity of the shingle method was determined to be approximately $1.1 \times 10^{-6} \text{ W cm}^{-1} \text{ }^\circ\text{K}$ compared to a blanket type insulation value $5 \times 10^{-7} \text{ W cm}^{-1} \text{ }^\circ\text{K}$.

Chapter 2: Fundamental Heat Transfer Process.

2. FUNDAMENTAL HEAT TRANSFER PROCESSES

Since the primary function of thermal insulation is to reduce heat flow through insulation, it is important to understand the various heat transfer processes responsible for this heat flow. These processes include conduction in the solid and gas phases and radiation exchange between surfaces, and in general they interact with each other in a complex manner. Free convection within the voids is always negligible even for the unevaluated insulations, since the characteristic length of the voids is so small (10-2 cm or less). Under certain conditions, however, they can be effectively decoupled and considered separately. The purpose of the present section is to review and to discuss the general fundamental aspects of each individual process in order to provide a basis for subsequent detailed consideration of heat transfer in a particular type of insulation.

2.1. Gas Conduction

The prominence of gas-conduction contribution is clearly demonstrated by the difference in thermal conductivity between unevaluated and evacuated insulations. The degree of vacuum required for desired insulation effectiveness is an important design problem for evacuated insulation, and can only be established by a careful consideration of gas conduction. Even for a highly evacuated insulation or insulations in a high-vacuum environment such as in outer space, out gassing and gas entrainment inside the insulation may render the gas-conduction contribution significant.

Heat conduction in gases is normally considered in separate molecular regimes (11): namely, free-molecule ($Kn > 10$), transition ($10 > Kn > 0.1$), temperature-jump (slip) ($0.1 > Kn > 0.01$) and continuum ($Kn < 0.01$), where Kn is the Knudsen number ($Kn = \lambda / L$) (λ the mean free path of molecular collisions, and L the characteristic length of the gas layer (e.g., the vacuum spacing). The various regimes have been under extensive investigations in the field of Rarefied gas dynamics, but these studies are mostly restricted to liberalized problems, i.e., $[(T_1 / T_2) - 1] \ll 1$, where T_1 and T_2 are temperatures of the two bounding surfaces. In extending these results to heat transfer calculations for cryogenic

insulations, however, care must be exercised since the boundary temperatures are often quite different, rendering the linearization condition invalid.

2.2. Solid Conduction

Conductive heat transfer through solid components of the insulation often constitutes the predominant mode of heat transfer in porous and multilayer insulations. To reduce or to eliminate the solid-conduction contribution is thus a major objective in the design of thermal insulation. Unfortunately, solid conduction cannot be easily reduced without affecting other heat transfer modes, particularly radiation, as well as many other mechanical and structural considerations. An excellent example of this dilemma is the Dewar flask, in which solid conduction is eliminated at the expense of structure integrity and relatively poor thermal effectiveness due to direct radioactive exchange. For zero-gravity applications, both conduction and radiation can probably be reduced through the use of loosely packed, floating particles. In general, however, reduction of solid conduction must be achieved by increasing thermal resistances to conductive heat flow. The logical way is, of course, to increase the effective length of heat flow paths and to decrease the effective flow cross-sectional area. This is best accomplished by creating tortuous and constricted conduction paths through the use of finely divided solid elements (particles, fibers, foams, screens, etc.) so that constriction resistances to heat flow are formed throughout the insulation.

Solid conduction in porous or multilayer insulations is a function of the thermal, mechanical, and geometric properties of the solid elements and the force acting on the insulation. The dependence of temperature is implicit in the force acting on the insulation. The dependence of temperature is implicit in the thermal and mechanical properties of the solid elements and the force acting on the insulation. The dependence of temperature is implicit in the thermal and mechanical properties. Among the inherent physical properties of the solid elements, thermal conductivity still exerts the major influence on thermal construction resistance. It should be emphasized that in the cryogenic temperature range the thermal conductivity of solids exhibits strong dependence of temperature as well as on molecular structure.

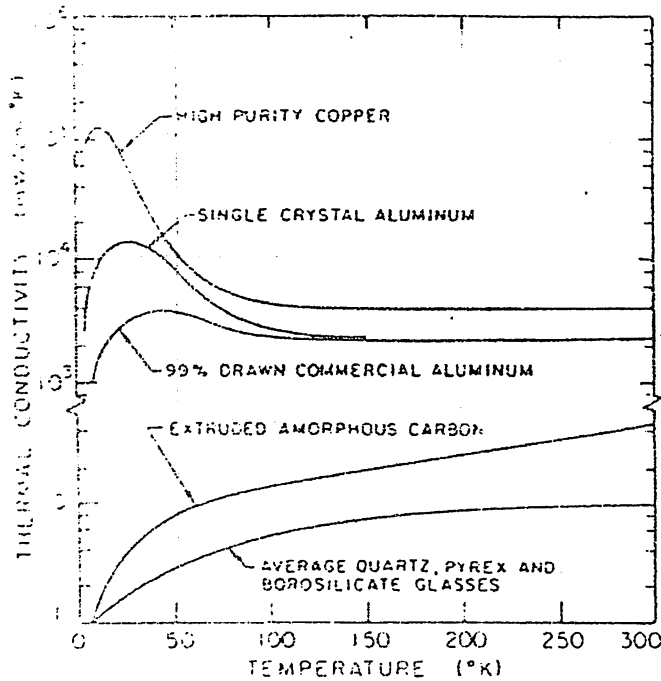


Fig 2.1 – Thermal Conductivities of low Temperature Solids.

In theory the thermal energy transport in solids is due primarily to two major mechanisms: mechanical interaction between molecules. (i.e., lattice vibrations) and translation of free conduction electrons. Because lattice vibrations can be treated as phonons, thermal transport in solids can be regarded as energy transport in phonon and electron gases, and the mean-free-path concept in the kinetic theory of molecular gases is directly applicable here. The free-electron contribution dominates in the energy transport in metals and the phonon contribution is predominant in dielectric solids, whereas in very impure metals or in disordered metals, the phonon contribution may be comparable with the free-electron contribution.

The disordered dielectrics with no free electrons and considerable lattice imperfection are the poorest solid conductors of heat, and consequently most porous or multilayer insulations are made of materials such as glass or polymeric plastics. Poor solid conductors, however, are also poor reflectors of radiation and are relatively ineffective for radiation shielding. A remedy is the use of metal particles dispersed in a dielectric medium as is evidenced in the opacified powders and in the aluminized plastic shields in multilayer insulations.

2.3. Radiation

Despite the fact that radiant energy involved at cryogenic temperatures is much smaller than that at room or high temperatures, radiation is still a major mode of heat transfer in cryogenic insulations.

The importance of the radiation mode is manifest in the large difference between the thermal effectiveness of ordinary porous insulations and that of multilayer insulations, in which radioactive exchange is greatly reduced by radiation shielding. Radioactive transfer refers to the transport of energy by electromagnetic waves and attenuation of radiation takes place in the forms of reflection, absorption, and scattering, all of which are essential elements in the heat transfer process in high-performance cryogenic insulations.

Chapter 3: Evacuated Multi Layer Insulation.

3. EVACUATED MULTILAYER INSULATION

The increasing demand for compact, light weight and highly effective thermal insulation for cryogenic applications has resulted in an impressive development and wide acceptance of evacuated cryogenic multilayer insulation systems. Great strides have been made in the last few years in understanding the complex heat transfer mechanisms involved. Reliable working formulas and computation techniques for heat transfer calculations are now available for thermal design and performance evaluation.

3.1. Thermo Physical Properties of Reflective Shields and Spacers

The importance of the thermo physical properties of insulation has been clearly demonstrated in the preceding section. In particular, advances in evacuated multilayer insulation have been made largely through the development of materials with optimal thermo physical properties. Furthermore, for reliable thermal design and performance evaluation which is crucial to all high-performance insulations, it is important to have at hand the correct values of thermo physical properties of the medium involved. This is especially the case in multilayer insulation since the basic elements of insulation (reflective shields and spacers) were developed not too long ago and relatively little information is available in the literature regarding its thermo physical properties. The primary thermo physical properties of the reflective shields and spacers that affect in a direct way the insulation heat transfer calculation are the thermal conductivity, specific heat, and radiation properties of the shields and the spacers.

3.2. Thermal Properties of Reflective Shields

The thermal conductivity of the reflective shield consists of contributions from the plastic film and the metal coating. For standard reflective shields such as Aluminized Mylar, the plastic contribution is small as compared to that due to metal. The thermal conductivity of metals at cryogenic temperatures has long been a subject of intensive

Studies, but most of these studies are concerned with bulk metals, in multilayer insulation, however, thin metal films are involved, and there might exist a substantial size effect in the heat transfer mechanism. The transport coefficients of thin films, such as electrical and thermal conductivities, are indeed expected to be less than those of the bulk metal, for some of the electron free paths will be shortened due to termination at the boundary surface. Since as the temperature decreases, phonon excitation (i.e., lattice vibration) will be reduced and the electron mean free path for the electron-phonon interaction will increase, the size effect is more pronounced at cryogenic temperatures.

3.3. Radiation Properties of Reflective Shields

The size effect is also expected in the radiation properties of thin metallic films as the absorption and emission of radiation of metals has its origin in electron motions. In addition to the similar size effect as in the conductivity case which is characterized by the ratio of two characteristic lengths, i.e., film thickness and electron mean free path, another effect comes into play in the radiation properties of metals as a result of one additional characteristic length, the field penetration depth. When radiation (i.e., a batch of electromagnetic waves) impinges on a metallic surface, the actual state within the distance into the metal. When the electron mean free path becomes large as compared to the penetration depth of the decaying field, such as is the case at Cryogenic temperatures, the electrons experience some effects due to the spatial variation of this field. These effects which are neglected in the ordinary free electron theory of absorption are given consideration in the ASE (anomalous-skin-effect) theory.

For practice, particularly in the thermal performance calculation for multilayer insulation where there exists a substantial difference in temperature among various shields, it is desirable to express total hemispherical Emissivity of the shield in a simple function of temperature. This is often approximated by

$$\epsilon = a T^b$$

Where constants a and b are prescribed on the basis of experimental information. For low-emittance metals, $b = 0.67$, while a may vary considerably in the range 10^{-3} to 10^{-4}

depending on the surface condition. For thin metallic films (e.g., aluminum on Mylar) at cryogenic temperatures, the calculation of radiation properties must incorporate both the size effect and the anomalous skin effect. Such a calculation has been made and a parallel experimental study has also been carried out. For the class of thin metallic films (about 400 Å thick aluminum or gold) actually used in Multilayer Insulation, there exists an appreciable effect of film thickness on the Emissivity. The thin film Emissivity increases with the decrease of thickness, and the effect becomes more pronounced at lower temperatures. For reflective shields with metallic layers coated only one side, such as the widely used singly aluminized Mylar, the plastic-side Emissivity of the shield must also be determined.

3.4. Normal Heat Transfer

Heat transfer in the direction normal to the layers often constitutes the major criterion in the thermal design and performance evaluation of multilayer insulation. The heat transfer mechanism involved is influenced by a large number of system parameters. The primary system parameters consist of the layer density (including thicknesses of insulation blankets and spacers, and the imposed pressure), radiation properties of the reflective shields and thermal properties (conduction, absorption, and scattering) of the spacer material.

The computation of normal heat transfer in multilayer insulation as a whole is always built on the calculation for a basic segment consisting of two neighboring shields, across which combined radiation and conduction (i.e., conduction through spacers or contact conduction in case of no spacers) takes place. For the spacer materials (including void) and thicknesses utilized in typical multilayer insulation systems, the optical thickness is very small compared to one, and the radiation and conduction contributions can be calculated separately. Furthermore, in the calculation of radiation contribution, the spacer effect can be neglected. The conduction contribution depends little on the thermal conductivity of the spacer layer but primarily on the interface contact conductance, which is in turn strongly influenced by the contact pressure.

Earlier treatments of normal heat transfer across evacuated cryogenic multilayer insulation have been a direct extension of the two-shield case to the multilayer system. This analytical approach stays closely with the discrete physical system, but the resultant computations, even with improved numerical techniques are cumbersome and the analysis is not flexible in its applications to a variety of physical situations.

3.5. Lateral Heat Transfer

In actual applications, heat flows inside the multilayer insulation system are seldom one dimensional in the normal direction. The complex geometry of the insulated system as well as penetrations by mechanical supports and plumbing often results in multidimensional heat paths and leaks. It would be a formidable problem to calculate the multidimensional heat transfer in such a highly anisotropic discrete medium as multilayer continuous model in the case of normal heat transfer to consider the multilayer insulation as a continuous, homogeneous but anisotropic medium with prescribed normal and lateral effective thermal conductivities. The definition of these effective conductivities may not be a one-dimensional normal or lateral case, must include the interaction effect between the normal and lateral heat transfer. No analysis or calculation of this nature has yet been reported.

Even the one-dimensional lateral heat transfer has not been easy for analysis and understanding. Until very recently, the lateral heat transfer had been regarded as governed solely by heat conduction in the thin metallized film on the plastic. Recent evidence, however, reveals that multiple reflections (i.e., lateral radiation tunneling) along two conducting films could affect the lateral heat transfer in a significant manner, especially when spacers are not used. The use of highly scattering fibrous spacers such as Tissuglas and Dexiglas reduces the lateral radiation contribution, but it takes a few layers of them to eliminate effectively this contribution.

While the use of spacers reduces lateral radiation transport, there are ways to reduce lateral heat conduction. The most effective technique is the selective slitting of insulation blanket to increase resistance in the direction of heat flow. The slitting results in a two

dimensional conduction problem that is tractable, but the resulting two-dimensional lateral conduction-radiation interaction becomes extremely complicated, more studies of the slitting effect on lateral conduction and conduction radiation interaction are needed.

Finally, it should be noted that the above discussion and analysis assume that the lateral and normal heat transfer are uncoupled. This is a valid approximation as long as the normal heat transfer is much smaller than the lateral heat transfer, i.e., only a very weak interaction between them exists. With various means of reducing the internal heat transfer such as using spacers and slitting, a stronger interaction might be resulted and the combined lateral and normal heat transfer must be analyzed. Unfortunately, the analysis will become so complicated that a reasonable solution of the analytical problem does not seem to be feasible at this time.

Chapter 4: Test Methods.

4. TEST METHODS

A variety of test methods and types of apparatus have been used to measure thermal properties of cryogenic insulations. Thermal conductivity is the most widely measured property; others which have been studied in some detail are specific heat, infrared radiation properties and out gassing characteristics of insulation materials. The discussion in this section will be limited to thermal conductivity test methods which have general applicability to evacuated powder fibers, foams, and multilayer insulations. Specific experimental details are contained in the cited references.

The thermal conductivity test methods may be divided into three general categories which are defined in terms of the methods used to measure the amount of heat transferred through the specimen. These are boil-off calorimetry, electrical input methods and indirect methods which use another property of the material or another solid material of known thermal conductivity for computation of specimen heat transfer. Boil-off calorimetry and electrical input are the most widely used methods, and they have been applied to all types of cryogenic insulations. The category of indirect methods which includes transient and heat flow meter procedures, has had more limited application than either of the other methods, and in general, does not have the accuracy of the others.

4.1. Boil-Off Calorimetry

As the name implies, the amount of thermal energy passing through the test specimen is determined from a measurement of the volume of gas vaporized from a fluid of known latent heat of vaporization at a constant temperature and pressure. The reservoir for this liquid forms the cold boundary of the specimen and a surface controlled at a higher temperature is located at the opposite specimen boundary to provide the driving potential. This warmer surface is generally heated either electrically or by a thermo stated fluid bath.

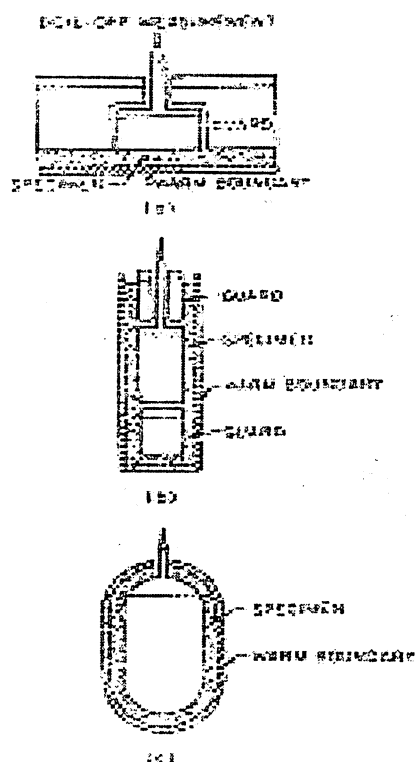


Figure 4.1 – Boil Off Calorimeter.

Cylindrical and flat-plate specimen geometries are those most commonly used. Spherical specimens have also been used, but it is difficult to obtain a uniform density for powders or to apply a layered insulation to this configuration. If the liquid reservoir is not totally enclosed by the test material, it is necessary to provide guard reservoirs adjacent to the measuring surface area so that only thermal energy from the specimen enters the measuring reservoir. The guard is filled with the same liquid and maintained at nearly the same temperature as the measuring fluid. The cold boundary temperatures are those attainable with a range of fluids typically from LH₂ at 20oK to butane at 273oK.

An early version of a calorimeter using the flat specimen geometry is the Wilkes device covered by ASTM C 420-62 T. The specimen is in the form of a disk approximately 25 cm in diameter. The measuring reservoir diameter is one-half of the specimen diameters, and it is surrounded by a guard vessel having an outer diameter equal to the specimen size. This guard also surrounds the measuring vessel fill and vent lines. The edges of the test specimen are additionally guarded with a loose-fill insulation to reduce heat transfer from the surroundings. A larger version of this calorimeter was

constructed for testing of insulation system for LH2-fueled hypersonic aircraft. The apparatus would accommodate a 1.5-m. diameter specimen up to 15-cm thick. The hot boundary temperatures have been achieved with a smaller device using LN2 as the calorimeter fluid for studying insulations applicable to cryogenically fueled entry vehicles. A further improvement in the flat-plate type of device is the so-called "double guarded" calorimeter. As filling of the guard reservoir disturbs the equilibrium conditions, which is more significant for LH2 because of its very low density, it is desirable to increase the time period between fills to a maximum. To accomplish this second guard vessel, filled with LN2, is placed exterior to the inner guard (filled with LH2) in order to reduce the exterior to the inner guard (filled with LH2) in order to reduce the extraneous heat transfer into this vessel. A larger version of this type of apparatus used for multilayer insulation testing is shown schematically in Fig.2. The large guard diameter is desirable because of the thermal anisotropy of multilayer insulations. The heater plate supports the insulation specimen and is movable so that thickness can be varied without removing the specimen or disturbing the temperature and vacuum conditions. This plate is also supported on a load cell for measuring the compressive pressure applied to the specimen.

Cylindrical calorimeters may be used for powder, fiber, foam, or Multilayer insulations. This type of apparatus shown below employs a cylindrical measuring vessel guarded either at the top only or at both ends. The specimen is placed in the annulus formed by the cryogen vessels and an outer controllable temperature cylinder or the vacuum enclosure. For porous materials, the lower guard may be eliminated. However, for multilayer which is very anisotropic, a lower guard reservoir is used to minimize two-dimensional heat transfer at the measuring area.

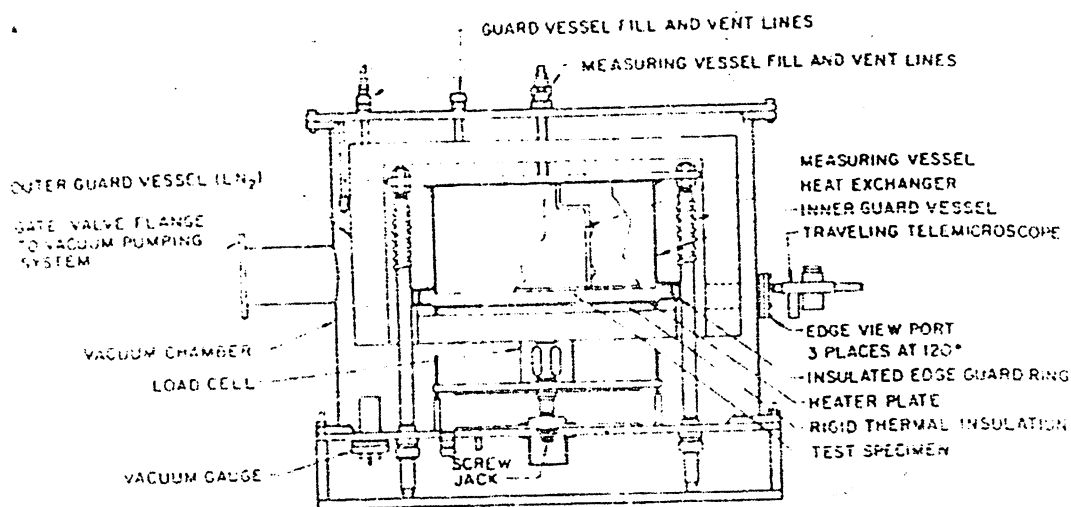


Figure 4.2 – Double guarded flat plate calorimeter.

In operating the boil-off calorimeter, care must be taken to minimize any extraneous heat transfer to the measuring reservoir such as through vent and fill lines. This is normally accomplished by thermally grounding these tubes to the guard vessel. In order to prevent condensation of vapor in the measuring section and its vent line, the temperature of the fluid in the measuring reservoir. This is done by maintaining the guard at a pressure 1 to 2 Torr above that of the test vessel. The rate at which the calorimetric fluid is vaporized is generally measured by a wet type of flow meter or a thermal mass flow meter. Constant reservoir pressures are maintained by use of pressure controlling valves referenced to a constant pressure sink.

An additional consideration in the testing of multilayer insulations, which applies to all methods, is the problem of two-dimensional heat transfer within the insulation. In order to assure one-dimensional conditions at the measuring area, the guard width to specimen thickness ratio must be sufficiently large. The minimum acceptable value is dependent upon the thermal conductivity normal to the layers and the ratio of normal to parallel conductivities, as well as the edge boundary temperature. For an edge temperature at the average of the hot and cold boundary temperatures, the ratio of guard width to thickness should be greater than fifteen.

CRYOGENIC INSULATION HEAT TRANSFER

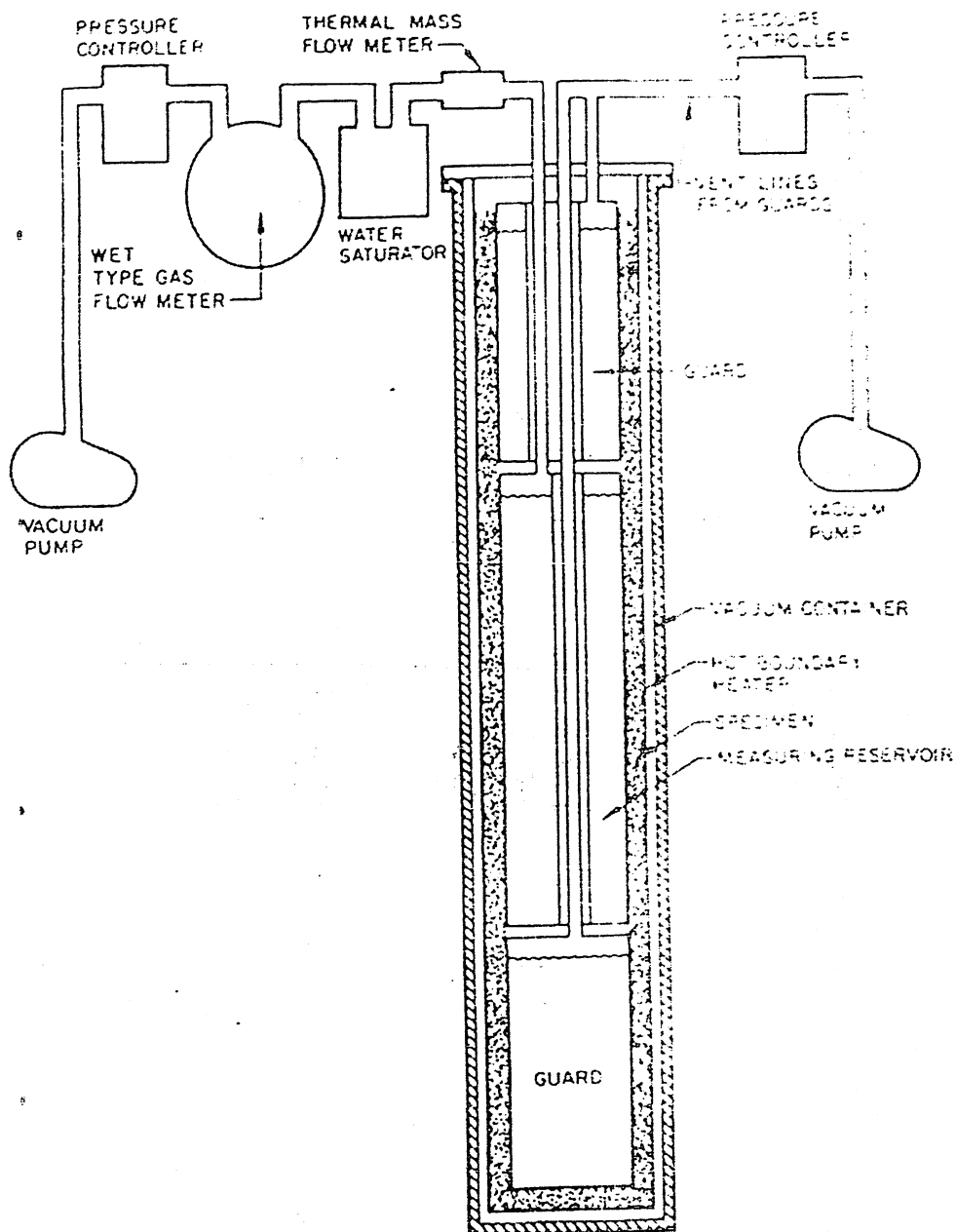


Figure 4.3 – Cylindrical Guarded Boil Off Calorimeter.

4.2. Electrical-Input Method

For this method the insulation heat flux is determined from a measurement of the electrical energy which is dissipated thermally in a resistive load uniformly distributed over the measuring area of the test specimen. Flat-plate or cylindrical geometries may be used for all types of insulations. The heated surface is located at the hot boundary of the specimen and a cryogenic fluid is used for the heat sink. No boil-off measurements are made so the cryogen reservoirs are not guarded. A guard heater is used to assure one dimensional heat transfer in the insulation measuring area and that all of the measuring heater power is transferred only through the insulation.

The classical example of the flat-plate type of apparatus is the guarded hot plate, ASTM C 177-63. For this method identical samples of the test material are placed at both surfaces of the guard-main heater plate arrangement, and heat sink plates which are at a lower temperature are located at the exterior surface of each specimen. The edges of this stack of sink-specimen heaters specimen sink are insulated with a loose fill material to reduce heat transfer to the surroundings. The guard heater power is adjusted to maintain a temperature balance between main and guard heater surface plates. Measuring heater power is assumed to be equally divided between both specimens. Examples of the use of this apparatus can be found else where.

Multilayer insulation tests have been conducted using a guarded cylinder method where in the insulation is wrapped on a cylindrical tube consisting of a central measuring heater with guard heaters at each end. The exterior surface of the insulation is in contact with or radiatively coupled to a cooled cylindrical heat sink.

4.3. Indirect Methods

Transient methods have been applied to multilayer and powder materials to measure insulation thermal diffusivity. The thermal conductivity is computed using known or estimated specific heat data and specimen density or weight. By this approach thermal conductivity can be studied for small temperature differences over a wide range of

boundary temperatures and with shorter measurement times than achievable by steady state methods. Comparative methods are also useful for some materials. In this case the specimen is placed between a heat source (heated electrically or by a fluid bath) and a material of known thermal conductivity which forms a heat flow meter at the cold boundary. This approach is not considered satisfactory for multilayer insulation because of the requirement for measurement of very small heat rates, and standard materials are not available in the low-conductivity range, for calibration. In general the indirect methods suffer from a poorer accuracy than the boil off or electrical input methods.

Chapter 5: Heat Transfer Model.

5. Heat Transfer Model

5.1. Introduction

The heat transfer in the Multi-Layer Insulation (MLI) consists of thermal radiation and thermal conduction. The thermal radiation is governed by the Radiative properties of vapor deposited aluminum coating on the polyester film. At the good vacuum condition, the thermal condition is governed by the thermal conductivity of spacer material and the contact heat transfer between the spacer and the reflective film. Studies shows that the conduction term in the heat transfer of MLI is governed by the contact heat by the contact heat transfer and not by the thermal resistance of spacer. In dimple type MLI that does not employ spacer material; thermal performance was superior to that of the MLI using polyester net space .The spacer will provide the contact thermal resistance at both sides of it. But spacer will add excess weight to MLI and is supposed to promote the contact heat transfer.

Transmissivity of thin aluminum layer from the plank's equation of black-body radiation shows that the Transmissivity is not negligible and increases at low temperature. Analyzing the heat transfer between two adjacent films and shows that the effect of non-zero Transmissivity of aluminum layer to the heat transfer is not negligible. In this study we analyze heat transfer in MLI considering the non-zero Transmissivity of aluminum coating of reflective film. In this situation, we have to consider the thermal radiation heat transfer from distant films in MLI. Employing Tsujimoto and Kunitomo's equation of Emissivity for aluminum in order to consider the temperature dependency.

In this study we analyzed heat transfer with constant heat transfer coefficient of contact between reflective layers. And the results of the analysis will be compared with the experimental data obtained from the vertical Cylindrical Calorimeter in that the compressive pressure is not affected by the gravity.

5.2. Transmissivity of Thermal Radiation of Very Thin Aluminum Layer

The thickness of vapor deposited aluminum on Insulation is about 300 to 900 Å. Transmissivity τ of thermal radiation through very thin aluminum layers is given by the equation.

$$\tau = (0.660 / T^4 \int_0^\infty (\exp(-4 * 10^4 D / \sqrt{\lambda}) (\lambda^5 (\exp(1.44 / \lambda T)))) \text{ ---- (1)}$$

Emissivity ϵ_0 and Reflectivity ρ are equated by τ as

$$\epsilon = \epsilon_0 (1 - \tau) \text{ ---- (2)}$$

$$\rho = \rho_0 (1 - \tau) \text{ ---- (3)}$$

$$\epsilon_0 + \rho_0 = 1. \text{ ---- (4)}$$

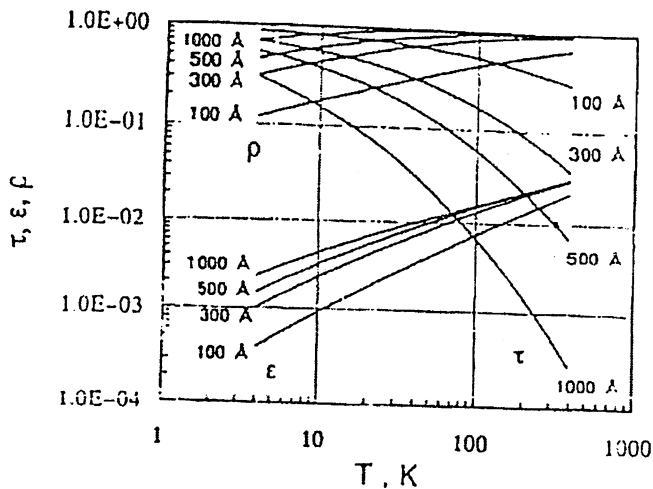


Figure 5.1 – Radiative Coefficients of Aluminum Thin Films.

Where ϵ_0 & ρ_0 are Emissivity and reflectivity for $\Gamma = 0$. For temperature dependency Tsujimoto and Kunitomo's equation of Emissivity for aluminum is

$$\epsilon_0 = 1.633 * 10^{-3} T^{0.495} \text{ ---- (5)}$$

estimated Transmissivity together with other optical properties for aluminum layers are shown above. Even at 500 Å thick aluminum layer, the Transmissivity is larger than 0.1 below 63k.

5.3. Multi Reflection of Radiation between Adjacent Layers.

We will now examine the transfer of Radiative power $e_i = \epsilon \sigma T^4$ which is emitted by the i-th layer and is multiply reflected between two layers at two different temperatures, T_i and T_{i+1} . By collecting terms of radiation absorbed by i+1 th layer, we will get the coefficient Ma_i which is a measure for the ratio of net absorption to e_i by i+1 th layer.

$$Ma_i = \epsilon_i (1 + \rho_i^2 + \rho_i^4 + \rho_i^6 + \dots) = (\epsilon_i / (1 - \rho_i^2)) \quad \text{----- (6)}$$

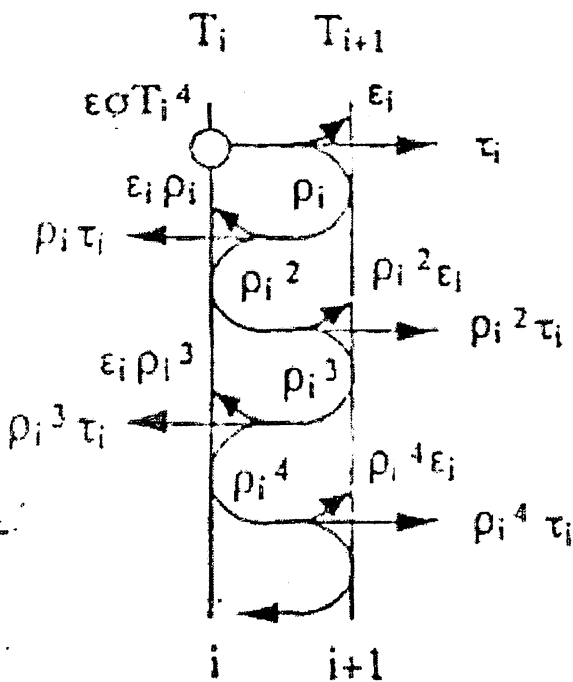


Figure 5.2 – Radiative Transfer between Adjacent Layers.

In the same way we will get Mt_i which is a measure for the ratio of net transmission to e_i beyond the i+1th layer to the right direction.

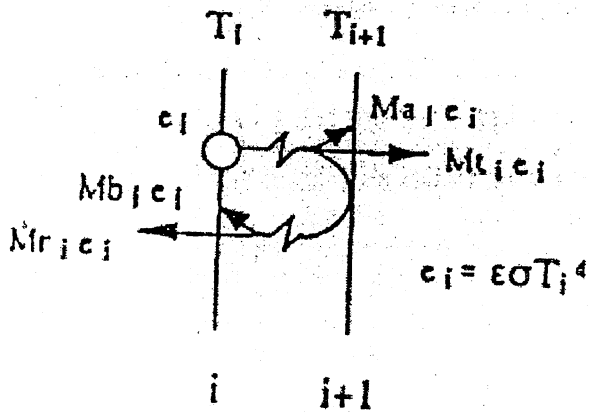
$$Mt_i = \tau_i (1 + \rho_i^2 + \rho_i^4 + \rho_i^6 + \dots) = (\tau_i / (1 - \rho_i^2)). \quad \text{----- (7)}$$

The coefficient Mr_i is a measure for the ratio of net transmission to e_i through the $i - th$ layer to the left direction and is expressed as

$$Mr_i = \tau_i \rho_i + \rho_i^3 \tau_i + \rho_i^5 \tau_i + \dots = (\tau_i \rho_i / (1 - \rho_i^2)). \text{----- (8)}$$

The coefficient Mb_i is a measure for the ratio of net absorption by the $i - th$ layer to the radiative power e_i and is expressed as

$$Mb_i = \rho_i \epsilon_i + \rho_i^3 \epsilon_i + \rho_i^5 \epsilon_i + \rho_i^7 \epsilon_i + \dots = (\rho_i \epsilon_i / (1 - \rho_i^2)) \text{----- (9)}$$

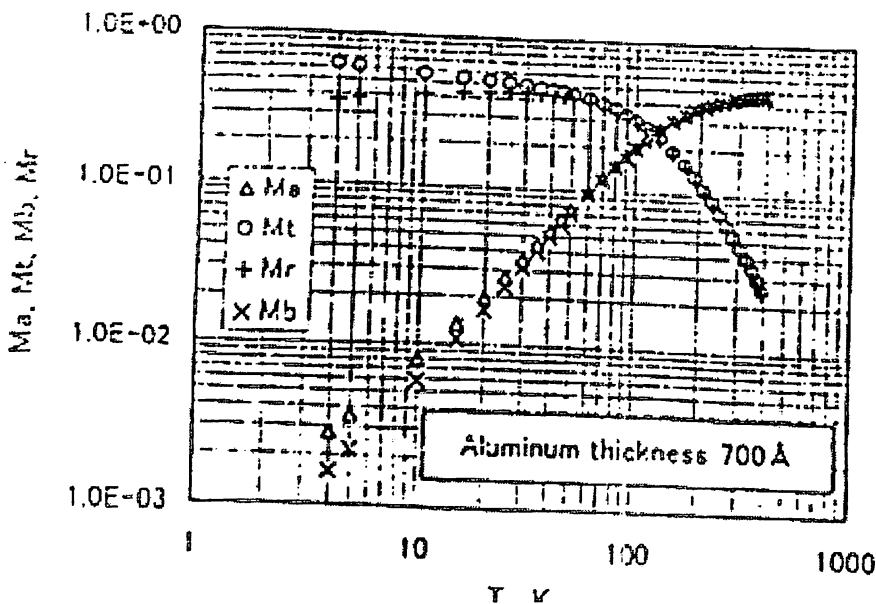


And one has an equation

$$Ma_i + Mt_i + Mr_i + Mb_i = 1. \text{----- (10)}$$

The Figure 5.3 below shows the heat transfer coefficient of Multi Reflection between two layers for the Aluminum layer of 700 \AA thick. When the Temperature of $i - th$ layer is lower than 100 K the ratio of radiation leak out from the cavity between the two layers becomes very large.

Figure 5.3 – Radiative Heat Transfer Coefficient of Multi Reflection Between Adjacent Two layers.



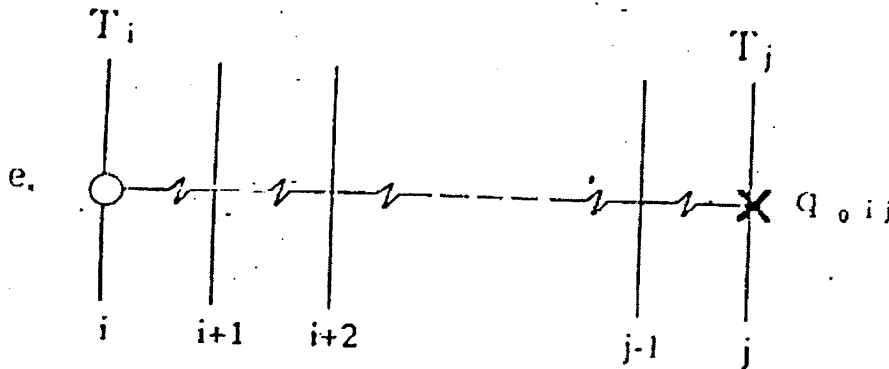
1 Heat Transfer Model.

5.4. Thermal Radiation from Distant Layers

We are analyzing the heat transfer in MLI that has N layers of Reflective films fabricated around the cold boundary ($i = 0$) at temperature T_0 (or T_c). The outermost layer ($i = N$) is surrounded by vacuum space and has no contact with the hot boundary wall ($i = N+1$) at temperature T_{N+1} (or T_H).

Thermal Radiation heat transfer from i th layer to j th layer after a series of Multi reflection between adjacent layers is considered.

Figure 5.4 – Radiative Heat Transfer Straight Forward radiation from i th Layer to $i + k$ th layer ($n=0$)



A part of the Radiative power $e_i = (\epsilon_i \sigma T_i^4)$, that is radiated from i th layer, is transmitted through the intermediate layers only once each and is absorbed by j th layer. We call this transfer the straight forward radiation heat transfer $q_{0 ij}$. we assume that the Radiative power attenuates by transmission through the reflective layers and that the reflective layers have no absorption band. Then the temperature of the radiation emitted from the i th layer remains constant through out the transfer. We can determine the radiative heat transfer coefficients of Multi reflection for this radiation Ma_i , Mt_i , Mri , and Mb_i by the temperature T_i throughout the transfer. Then the straightforward radiation heat transfer $q_{0 ij}$ is now expressed as

$$q_{0 ij} = Mt_i^{(K-1)} Ma_i e_i \quad \dots \quad (11)$$

where $K = (j-i)$

The number of layers through which q_{0ij} is transmitted is $K-1$. We consider the transfer path in which the number of layers is larger than $K-1$ by n .

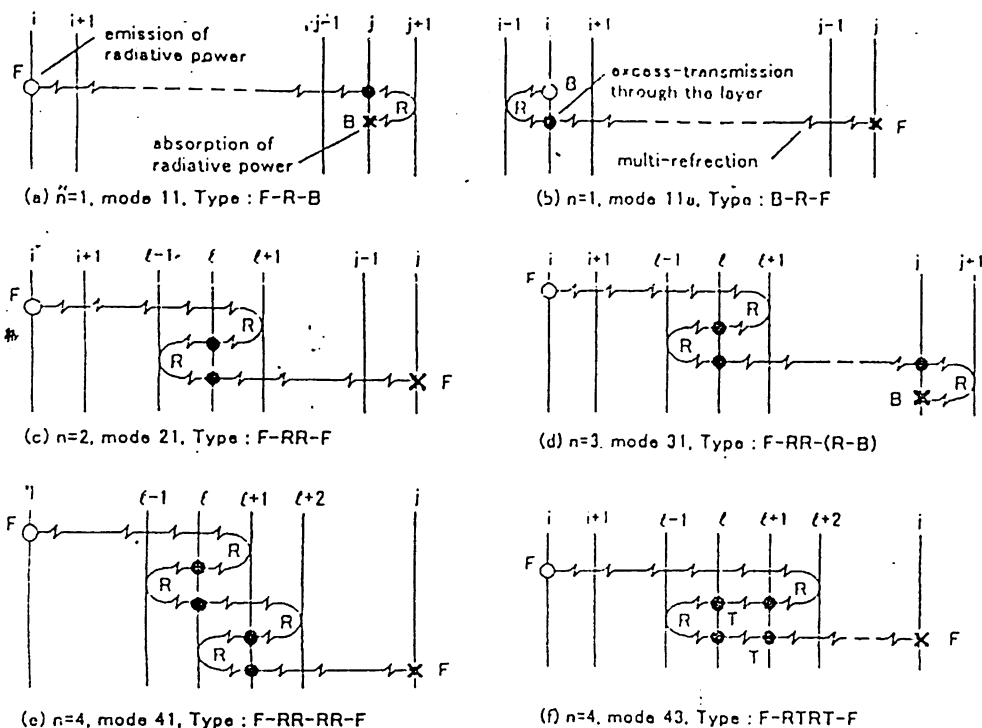


Figure 5.5. Radiative Heat Transfer from i th Layer to $i + k$ th layer ($n > 0$)

In case of $n = 1$ there are two modes of transfer path, mode 11 and mode 11_a shown below in 5 (a) and (b) respectively. These two modes are symmetrically each other. In mode 11 the radiative power is emitted forward (F) to j th layer, is returned (R) and incidents backward (B) to j th layer. The transmission pattern for mode 11 is expressed as F – (R-B). The radiation heat transfer for mode 11 and mode 11_a can be expressed by using the straightforward radiation heat transfer as follows respectively.

$$q_{11ij} = B_{11} * q_{0ij} \quad \text{----- (12)}$$

$$q_{11a ij} = B_{11a} * q_{0ij} \quad \text{----- (13)}$$

Where B_{11} and B_{11a} are the transfer operators B mode for mode 11 and mode 11_a respectively and are expressed as follows.

$$B_{11}, B_{11a} = M_{ri} \quad \text{----- (14)}$$

From equations (12) and (13) the expression for the thermal radiation heat transfer for $n = 1$

is given the transfer operator B_n for $n = 1$.

$$q_{1ij} = B_1 \cdot q_{0ij} \quad \text{----- (15)}$$

$$B_1 = B_{11} + B_{11a} = 2 M_{ri} \quad \text{----- (16)}$$

The pattern of transfer path and the transfer operator B mode for $n = 1$ to 7 is summarized in Table 1.

For mode 43 the transfer path change its direction at $l + 2$ th layer, transverses through $l + 1$ th layer and l th layer changes its direction again at $l - 1$ th layer and then goes to j th layer. The pattern of transfer path form mode 43 is expressed as $F - RTRT - F$ where the number of transverses path (T) is even. The first change of direction (R) in the path can be located at the layers from $i + 1$ to $j + 2$. As the number of the location is $K + 2$ the transfer operator for mode 43 is expressed as,

$$B_{43} = (K + 2) M_{ri}^2 M_{ti}^2 \quad \text{----- (17)}$$

TABLE 1. Mode of Radiative Heat Transfer Path from i-th Layer to j-th Layer

n	T	R	mode	pattern of path	B mode $k= i-j $	symmetrical mode		
1	0	1	11	F-(R-B)	B11 = Mr_i	11a		
2	0	2	21	F-RR-F	B21 = $(k+1) Mr_i^2$	-		
			22	(B-R)-(R-B)	B22 = Mr_i^2	-		
3	0	3	31	F-RR-(R-B)	B31 = $(k+1) Mr_i^3$	31a		
			32	F-(TRT-B)	B32 = $Mr_i Mt_i^2$	32a		
4	0	4	41	F-RR-RR-F	B41 = $1/2! (k+1)(k+2) Mr_i^4$	-		
			42	(B-R)-RR-(R-B)	B42 = $(k+1) Mr_i^4$	-		
			43	F-RTRT-F	B43 = $(k+2) Mr_i^3 Mt_i^2$	-		
			44	(B-R)-(TRT-B)	B44 = $Mr_i^2 Mt_i^2$	44a		
5	0	5	51	F-RR-RR-(R-B)	B51 = $1/2! (k+1)(k+2) Mr_i^5$	51a		
			52	F-RR-(TRT-B)	B52 = $(k+1) Mr_i^3 Mt_i^2$	52a		
			53	F-RTRT-(R-B)	B53 = $(k+1) Mr_i^3 Mt_i^2$	53a		
			54	F-(TRT-B)	B54 = $Mr_i Mt_i^4$	54a		
6	0	6	61	F-RR-RR-RR-F	B61 = $1/3! (k+1)(k+2)(k+3) Mr_i^6$	-		
			62	(B-R)-RR-RR-(R-B)	B62 = $1/2! (k+1)(k+2) Mr_i^6$	-		
			2	4	631	F-RR-RTRT-F	B631 = $1/2 (k+2)(k+3) Mr_i^4 Mt_i^2$	-
					632	F-RTRT-RR-F	B632 = $1/2 (k+2)(k+3) Mr_i^4 Mt_i^2$	-
			4	2	64	(B-R)-RR-(TRT-B)	B64 = $(k+1) Mr_i^4 Mt_i^2$	64a
					65	F-RTTRT-F	B65 = $(k+3) Mr_i^2 Mt_i^4$	-
7	0	7	66	(B-TRT)-(TRT-B)	B66 = $Mr_i^2 Mt_i^4$	-		
			67	(B-R)-(TRT-B)	B67 = $Mr_i^2 Mt_i^4$	67a		
			71	F-RR-RR-RR-(R-B)	B71 = $1/5! (k+1)(k+2)(k+3) Mr_i^7$	71a		
8	0	8	72	F-RR-RR-(TRT-B)	B72 = $1/2! (k+1)(k+2) Mr_i^3 Mt_i^2$	72a		
			731	F-RR-RTRT-(R-B)	B731 = $1/2! (k+1)(k+2) Mr_i^3 Mt_i^2$	731a		
			732	F-RTRT-RR-(R-B)	B732 = $1/2! (k+1)(k+2) Mr_i^3 Mt_i^2$	732a		
			74	F-RTRT-(TRT-B)	B74 = $(k+1) Mr_i^3 Mt_i^4$	74a		
9	0	9	75	F-RR-(TRT-B)	B75 = $(k+1) Mr_i^3 Mt_i^4$	75a		
			76	F-(TRT-B)	B76 = $Mr_i Mt_i^6$	76a		

Left side F in the pattern of path means forward emission. Left side B means backward emission.
Right side F means forward incident. Right side B means backward incident.

5.5. Radiative Heat Transfer at the boundary.

The boundary wall is usually made by polished stainless steel and its Transmissivity of radiation is Zero. Taking this condition into account, the Radiative heat transfer coefficient of Multi – reflection must be corrected at the boundaries and the layers close to the wall. For the Radiative power emitted by the cold wall, the coefficients of Multi-Reflection between the cold boundary and the first layer of MLI are modified as Ma_c , Mt_c , Mr_c in Figure 6 below. By using the reflectivity $\rho_c(T_i)$ and the emissivity $\epsilon_c(T_i)$ of the cold boundary.

For the Radiative power emitted from the i – th layer in MLI the coefficients of Multi reflection are modified as $Ma_{i,c}$, $Mt_{i,c}$, $Mr_{i,c}$ in figure 6. The same modification must be done at the hot boundary.

As the Transmissivity of the boundaries is Zero some of the heat transfer path is not realized. For the mode 11, the transfer operator defined operator defined by equation (12) and (14) is corrected for $j = 0$ as equation (18) and is corrected for $j = 1$ as equation (19).

Multi Reflection of Thermal Radiation at the Cold boundary wall.

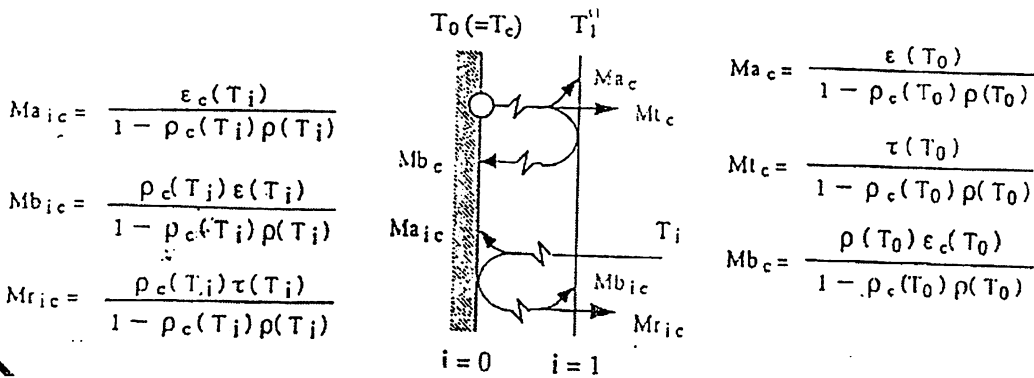


Figure 5.6. Multi Reflection of Thermal radiation at the boundary.

$$B_{11i0} = 0 \quad \text{-----} \quad (18)$$

$$B_{11i1} = Mr_{ic} \quad \text{-----} \quad (19)$$

5.6. Energy Balance of the Layer

Total Radiative heat transfer from i th layer to j th layer q_{tij} is described by equation (20). In the equation B_{nij} for large n can be neglected because the attenuation is large.

Total radiation energy emitted by all layers including the cold and hot boundary other than i th layer and then absorbed by the i th layer is described by the equation (21). Total Radiative energy emitted by the i th layer and absorbed by other layers is described as equation (22).

$$q_{tij} = (1 + \sum_{n=1}^{\infty} B_{nij}) q_{0ij} \quad \text{-----} \quad (20)$$

$$q_{I_i} = \sum_{j=0}^{N+1} q_{tji} \quad (j \text{ not equal to } i) \quad \text{---} \quad (21)$$

$$q_{O_i} = \sum_{j=0}^{N+1} q_{tj} \quad (j \text{ not equal to } i) \quad \text{----} \quad (22)$$

Then we have the energy balance of the i th layer for the steady state as

$$q I_i + h_c (T_{i+1} - T_i) = q O_i + h_c (T_i - T_{i-1}) \text{ ----- (23)}$$

Where the contact heat transfer coefficient h_c ($W/m^2 K$) between the adjacent layers is assumed to be constant for all the layers. With this assumption h_{c_n} is zero because we assume that the outer most layer of MLI ($i = N$) has no contact with the hot boundary wall. The heat transfer at the cold boundary ($i = 0$) and the heat transfer at the hot boundary are equivalent to the overall heat transfer through the MLI q (W/m^2) that is described as

$$q = q I_o + h_c (T_1 - T_0) - q O_o = q O_{N+1} - q I_{N+1} \text{ ----- (24)}$$

5.7. Analytical results and Comparisons with the Experiment

The energy balance equations (23) and (24) for each layer in MLI that has 40 layers of reflective films are numerically solved for two temperature condition of boundary wall, Case L ($T_c = 4.2 K$, $T_h = 77 K$) and Case H ($T_c = 77 K$, $T_h = 300 K$). The relations between the heat transfer q (W/m^2) through the MLI and the contact heat transfer coefficient h_c (W/m^2K) through the MLI and the contact heat transfer coefficient h_c (W/m^2K) were obtained for the different thickness of Aluminum layer from 300 \AA to 3000 \AA (figure 7). The Emissivity for the boundary wall is estimated by the equation

$$\epsilon_i = 1.58 * 10^{-2} T^{0.355} \text{ ----- (25)}$$

This is approximated from the data for mechanically polished stainless steel obtained experimentally. In our analytical calculation the radiation transfer path for n from zero to seven were taken into account. The net heat transfer q comes close to an asymptotic value by increasing the number n (Figure 8). In case L when the Transmissivity of radiation is large the analytical result for the aluminum thickness of 700 \AA shows that it is enough to consider n up to seven. But for the case of Aluminum thickness of 300 \AA the radiation does not attenuate so much at such a low temperature. We may need to take the radiation transfer path for n larger than seven in to account to obtain the convergence of analytical result. The relationship between q and h_c shown in figure 7 has a shape of character S. for

large value of h_c the effect of thermal barrier by the vacuum space surrounding the MLI constraints the net heat transfer and makes the curve flat. For small value of h_c , heat transfer is governed by thermal radiation and stays constant for h_c . The thermal performance of MLI is limited in those two horizontal lines.

The effect of aluminum layer thickness to the thermal performance of MLI is also shown in Figure 7. The heat transfer q is not decreased significantly for the thickness larger than 700 \AA in case H and for larger than 1500 \AA in case L. Effect of Aluminum coating thickness on Double Aluminized Mylar; Mylar film aluminized on both sides from 350 \AA per side to 600 \AA per side at the boundary temperatures 20 K and 80 K . No significant effect on overall thermal performance was shown earlier. Our analytical results in figure 7 show very little difference in the heat transfer between the aluminum thickness of 700 \AA and that of 1200 \AA for the temperature condition in Case H. In case L the difference cannot be neglected but it might be very small for the case when T_c is 20 K . Thermal performance data for the MLI samples which do not employ spacer material is obtained from cylindrical Calorimeter. The heat transfer levels of the test data are drawn as horizontal lines with symbols at the both the ends so as to cross the theoretical curve.

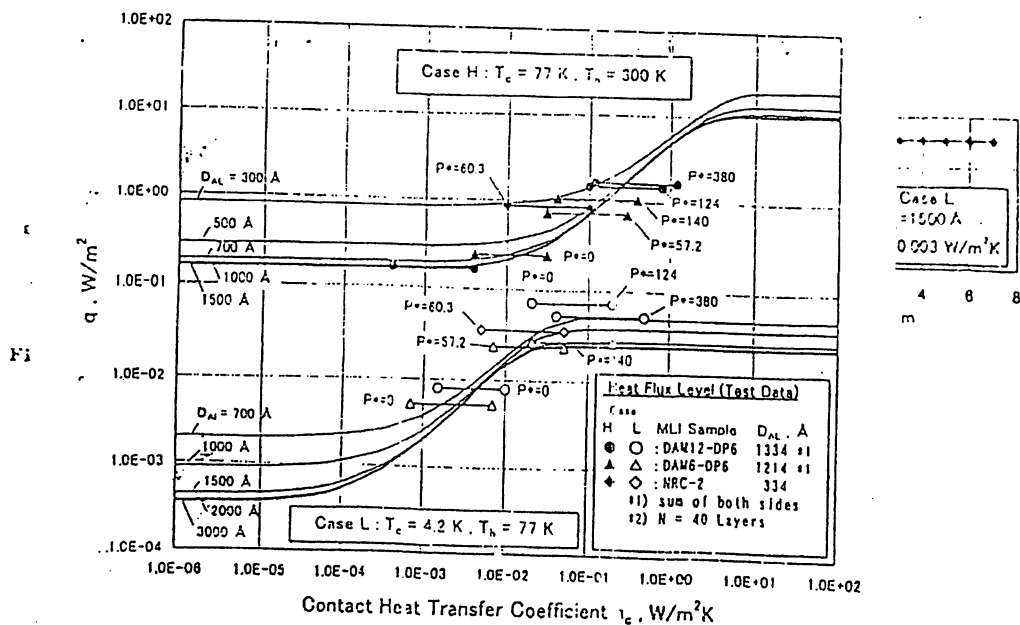


FIGURE 7. Thermal performance q of MLI and contact heat transfer coefficient h_c between adjacent layers

Figure 5.7. Thermal Performance q of MLI and h_c

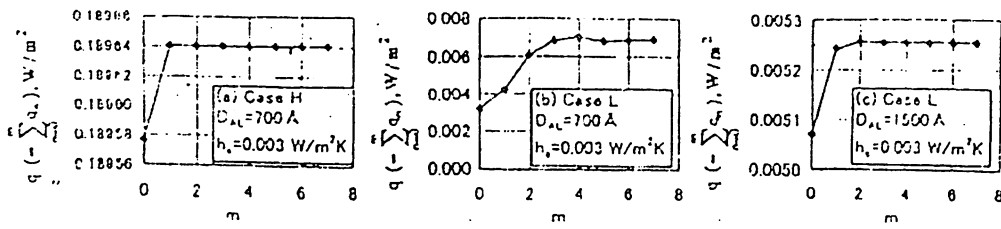


Figure 5.8. Calculated Values of net heat flux by increasing n .

The test data were obtained for the condition of compression in the MLI from Zero to the Level at which the increase in compression will not give a significant promotion in heat Transfer. It is found that the heat transfer coefficients h_c for Case H are larger than that for Case L by factor 2 to 4.5. This shows that there is a temperature dependency in h_c .

Chapter 6: Conclusion.

6. Conclusion

A method to solve the heat transfer through the MLI analytically is developed when thermal radiation Transmissivity of the reflective film is not negligible. The relations between the heat transfer and the contact heat transfer coefficient between adjacent layers are evaluated for two boundary temperature conditions. The thickness of the Aluminum layer to get a good thermal performance is obtained for each boundary temperature condition. In order to obtain the exact relation between the contact heat transfer coefficient and the compressive pressure additional investigation about the temperature distribution in MLI will be needed.

Reference

1. The Effect of Non-Zero Thermal Radiation Transmissivity of the Aluminized Mylar Film on the Thermal Performance of Super-Insulation.

T.Ohmori, A. Yamomoto, and M. Nakajima.

Ishikawajima Harima Heavy Industries Co.Ltd, (IHI)
Koto – ku , Tokyo 135 – 8732, Japan.

High Energy Accelerator Research organization (KEK)
Tsukuba, Ibaragi, 305 – 0801, Japan.

2. Cryogenic Insulation Heat Transfer

Cunnington & Tien. University of California, Berkeley.

3. Transport Phenomena

Bird, Stewart & Lightfoot.

John Wiley & Sons.